



ELSEVIER

Palaeogeography, Palaeoclimatology, Palaeoecology 172 (2001) 283–296

**PALAEO**

www.elsevier.com/locate/palaeo

# Controls on isotopic chemistry of the American oyster, *Crassostrea virginica*: implications for growth patterns

D. Surge<sup>a,\*</sup>, K.C. Lohmann<sup>a,1</sup>, David L. Dettman<sup>b,2</sup>

<sup>a</sup>Department of Geological Sciences, University of Michigan, 2534 C.C. Little Building, 425 E. University Avenue, Ann Arbor, MI 48109-1063, USA

<sup>b</sup>Department of Geosciences, University of Arizona, Tucson, AZ 85721, USA

Received 19 June 2000; accepted for publication 9 May 2001

## Abstract

The American or eastern oyster, *Crassostrea virginica*, can potentially serve as a recorder of environmental change in estuarine habitats. However, before oysters can confidently be used to reconstruct past variation in salinity and temperature in coastal environments, relations between modern shell chemistry and ambient salinity and temperature must be understood. Samples from the resilifer on the surface of the hinge (foliated calcite) and in cross-section (foliated and chalky layers) have very similar isotopic composition, implying that all three areas respond identically to ambient water conditions. More detailed sampling focused on the chalky layer because this region exhibits maximum shell extension which allows for high-resolution sampling. Water temperature, salinity,  $\delta^{18}\text{O}_{\text{WATER}}$ , and the  $\delta^{13}\text{C}_{\text{DIC}}$  (dissolved inorganic carbon) were measured in Blackwater River, near Naples, Florida, from June 1997 to November 1999 to construct a predicted model shell against which the observed isotopic data from live-collected oysters were compared. From these data, it was determined that *C. virginica* precipitated its shell near isotopic equilibrium. Values of  $\delta^{13}\text{C}_{\text{SHELL}}$  follow the general trend of the predicted equilibrium model with a positive offset of  $\sim 1\%$  during cold winter months. Variation in growth rate or incorporation of a higher percentage of metabolically derived carbon may explain the degree of offset. *C. virginica* from southwest Florida does not appear to deposit shell when water temperature is above  $\sim 28(\pm 2)^\circ\text{C}$ , though the influence of temperature versus gametogenesis attributing to the slowing down of shell accretion cannot be deconvoluted. Importantly, there is no consistent pattern between the location of dark, translucent growth bands and peaks or valleys on the profile of isotopic composition of the shell. Therefore, these growth structures cannot be used as independent proxies of growth season, tides, lunar phase, or shell age. © 2001 Published by Elsevier Science B.V.

**Keywords:** Mollusca; Bivalvia; Carbon; Oxygen; Ecology; Florida

## 1. Introduction

The dynamic nature of coastal environments influences the character of ecological habitats and is impacted by climate along the continental margin. In particular, estuarine water has variable salinity due to the mixing of meteoric surface runoff from land and ocean water. Estuarine salinity variation can be influenced by seasonal changes in rainfall, tidal currents,

\* Corresponding author. Fax: +1-734-763-4690.

Present address: Iowa State University, Department of Geological & Atmospheric Sciences, 253 Science I, Ames, Iowa 50011-3212.

E-mail addresses: dsurge@umich.edu (D. Surge), kacey@umich.edu (K.C. Lohmann), dettman@geo.arizona (D.L. Dettman).

<sup>1</sup> Fax: +1-734-763-4690.

<sup>2</sup> Fax: +1-520-621-2672.

stratification, and local circulation patterns (Kjerfve, 1989). Moreover, many coastal areas are highly populated and therefore, are subject to stresses of human activity. For example, many estuaries from southern Florida have been affected negatively by changes in watershed drainage with the building of canal systems constructed to increase areas available for agriculture and residential development. Some estuaries receive larger amounts of freshwater runoff due to channelization, as well as increased nutrients from agricultural lands and sewage. Channelization can also create elevated salinity in neighboring estuaries when the natural drainage pattern and runoff is diverted. Organisms currently inhabiting these estuarine habitats are able to accommodate the increased variability of environmental conditions. To reconstruct past changes in ecological and climate patterns associated with coastal settings, we must first develop an approach that will accommodate the inherently dynamic nature of environments at the land-sea interface and the animals that live there.

Many studies that reconstruct past environments look to the isotopic compositions and elemental concentrations of skeletal carbonate of aquatic organisms (Mook, 1971; Jones, 1983; Spero, 1990; Jones and Allmon, 1995; Bemis and Geary, 1996; Jones, 1996; Jones and Quitmyer, 1996; Klein et al., 1996a,b; Swart et al., 1996; Dettman et al., 1999). Jones (1983) pioneered the utility of sclerochronologic records in the shells of molluscs and combined morphologic features (e.g. growth banding) with carbon and oxygen isotopes to reconstruct seasonal environmental change (e.g. Jones et al., 1984; Jones, 1996; Jones and Allmon, 1995; Jones and Quitmyer, 1996). Despite the presence of an isotopic and chemical record, however, it is difficult to quantitatively relate shell chemistry to surface water salinity and temperature of coastal settings. For example, even though  $\delta^{18}\text{O}_{\text{CALCITE}}$  can often be used to determine open marine paleotemperatures, it is difficult to apply this approach in coastal and estuarine environments because of high frequency variation of both salinity and temperature. In such settings, change in water temperature cannot be easily discriminated from change in salinity and  $\delta^{18}\text{O}_{\text{WATER}}$ . Thus, additional constraints, such as ecological/metabolic considerations (e.g. hibernation temperature) or elemental

proxies of temperature or salinity, must be employed to decipher these environmental records.

This study seeks to understand the controls on isotopic chemistry of shell carbonate for the American or eastern oyster *Crassostrea virginica* and then quantify the relationship between the isotopic composition of its shell and ambient water conditions. *C. virginica* is the dominant bivalve in many estuaries along the eastern seaboard of North America, and therefore, has the potential to be a valuable recorder of environmental change at the land-sea interface. Furthermore, *C. virginica* is ideal for reconstructing the environment of coastal settings because of its cosmopolitan occurrence across a broad salinity gradient, its latitudinal and geologic range, and its incremental growth pattern. By examining chemical records from multiple shells, we can reconstruct average conditions characteristic of this region.

To better understand controls on shell chemistry, we first examined whether there are differences in  $\delta^{18}\text{O}$  and  $\delta^{13}\text{C}$  in the various microstructural areas (foliated versus chalky) of shell carbonate. We tested the hypothesis that the isotopic composition of microstructural areas are statistically indistinguishable because one area may more faithfully record ambient conditions than another. After examining shell microstructure, shell chemistry was calibrated with water chemistry. Kirby et al. (1998) suggested that *C. virginica* precipitates its shell near oxygen isotope equilibrium. We more precisely test this hypothesis using high-resolution data on temporal variation in water chemistry and environmental conditions coupled with microsampling methods to provide subannual resolution of shell chemistry. High-resolution data were also used to test whether *C. virginica* is in isotopic equilibrium with respect to  $\delta^{13}\text{C}$  of dissolved inorganic carbon. We first characterized water chemistry by examining mixing relations between meteoric and marine waters, changes that occur seasonally. This information allowed us to test the hypothesis that *C. virginica* precipitates its shell in isotopic equilibrium with the water in which it grows. Once shell chemistry is understood, ontogenetic questions can be addressed. By comparing measured isotopic compositions of shell carbonate with that of a predictive model, seasonal changes in shell growth rate were investigated. Finally, Kirby et al. (1998) and Andrus and Crowe (2000) suggested that certain

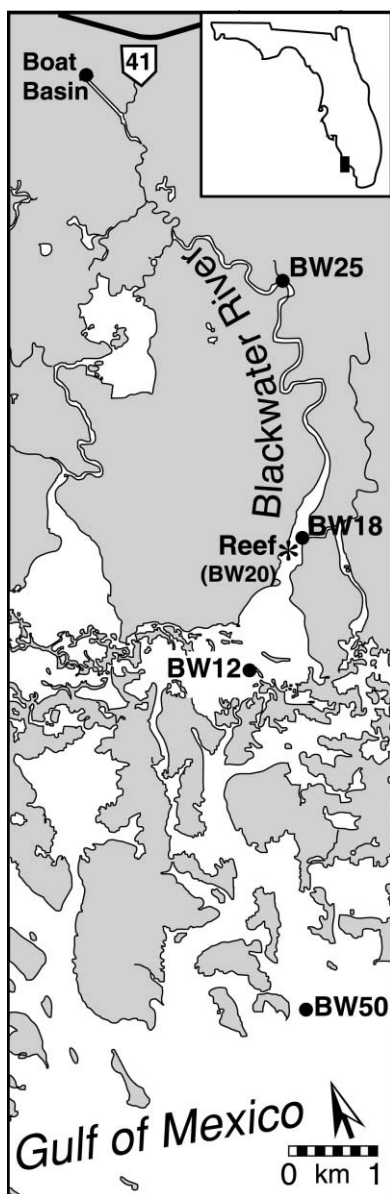


Fig. 1. Map of the study area indicating the 6 sampling sites along a 12 km transect. Shaded areas are covered by mangrove forest and unshaded areas represent water ways. Monthly water samples for isotopic analyses and temperature, salinity, and pH measurements were taken at each site. Hourly data (temperature and salinity) were measured at and shells were collected from the oyster reef at BW20 in Blackwater River.

morphologic features on the shell of *C. virginica* can be used to independently identify season of growth. We compared the location of dark, translucent growth bands with the isotopic records of growth season, tides, and lunar phase to assess any correlation.

## 2. Study area

This study focuses on Blackwater River, which is situated near Naples, Florida along the northernmost extent of the Ten Thousand Islands west of the Everglades (Fig. 1). Estuaries in this region are marine dominated and affected markedly by seasonal freshwater input. Tidal range averages 0.6 m and estuary waters are mixed semidiurnally (McIvor and Smith, 1995). Estuaries with undisturbed watersheds are vertically well-mixed, having very little difference in salinity, temperature, and pH through the water column. Surge and Lohmann (2001, in preparation) provide a more detailed discussion regarding the chemical hydrology of this area.

Blackwater River is, as its name implies, a typical black-water river, approximately 12 km in length, with a blind source that was originally in a salt-water marsh. A boat ramp has since been constructed at its most upstream extent. The black, tea-colored water results from input of large amounts of humic material from the mangrove leaf litter. Blackwater River has a relatively undisturbed watershed forested by red, black, and white mangroves (*Rhizophora mangle*, *Avicennia germinans*, and *Laguncularia racemosa*, respectively). In its lower extent, it contains oyster reefs that form islands on which new mangrove forests develop. Most of the oyster reefs are emergent at low tide. We focused on one oyster reef locality for this study, and established 6 sites along a transect from the most upstream portion of Blackwater River down to the Gulf of Mexico to characterize mixing relations between marine and meteoric water that ultimately influence oyster shell chemistry (Fig. 1).

## 3. Water properties and chemistry

Physical and chemical water properties (temperature, salinity, carbon and oxygen isotopes) were measured/sampled along a spatial gradient between

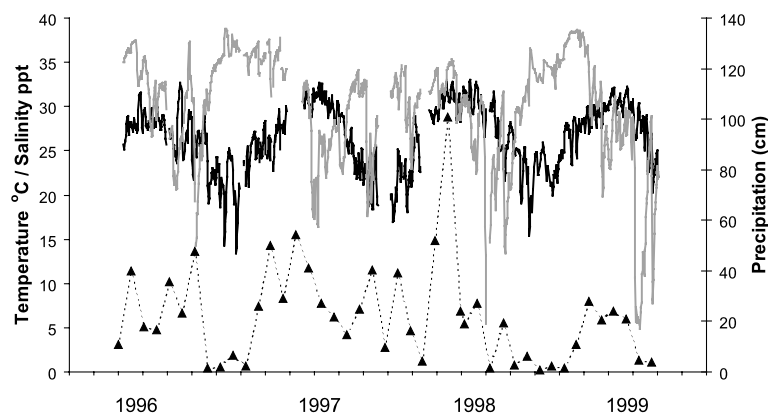


Fig. 2. Salinity, temperature, and precipitation for years 1996–1999. Black line = temperature ( $^{\circ}\text{C}$ ); gray line = salinity (ppt); diamonds with dashed line = precipitation (cm of total accumulation per month). Temperature and salinity measurements taken at the oyster reef (site BW20) from April 1996 to November 1999. Daily averages were reduced from hourly measurements. Precipitation measured at Naples and Fort Meyers, Florida, courtesy of the National Oceanographic and Atmospheric Administration.

freshwater and marine sources, and at two temporal scales (hourly and monthly). Hourly water property data were collected from the oyster reef locality using a YSI data logger equipped with depth, temperature,

and salinity probes that was moored at the reef where oysters were harvested. This provided high-resolution data on ambient water conditions with relatively high precision. Salinity and temperature measurements at this site were collected over a 44-month period from April 1996 to November 1999 (Fig. 2).

Table 1

Temperature and salinity measured monthly at site BW20

Date collected	Temperature ( $^{\circ}\text{C}$ )	Salinity (ppt)
7/28/97	31.08	24.2
10/15/97	26.13	29.0
12/17/97	19.93	23.3
1/14/98	23.62	30.3
2/17/98	26.35	30.5
3/23/98	20.33	26.9
4/24/98	25.60	31.4
5/21/98	29.91	34.0
6/24/98	31.20	34.4
7/23/98	30.67	30.2
8/24/98	31.70	25.9
9/22/98	30.80	16.2
10/21/98	28.80	21.6
11/17/98	27.00	22.6
12/17/98	19.70	30.3
1/28/99	19.70	35.5
2/24/99	17.57	34.4
3/30/99	25.00	35.4
4/30/99	28.34	36.6
5/28/99	30.85	36.3
6/27/99	29.87	32.3
7/27/99	32.72	28.2
9/8/99	30.78	29.9
10/7/99	27.69	12.3
11/18/99	No data	23.3

In addition to hourly measurements, temperature, salinity, and  $\delta^{18}\text{O}_{\text{WATER}}$  were determined monthly from 6 sites along a 12 km transect to constrain seasonal variation in these parameters (Fig. 1). These measurements and samples were taken during high tide at roughly the same day in a lunar cycle (during the week of a full moon) to minimize any variation that might be influenced by changing tides. A hand-held Hydrolab data logger, equipped with depth, temperature, and salinity probes, was employed to take monthly measurements at each site over a 25-month period from July 1997 to November 1999 (Table 1). The temperature and salinity probes for the YSI and Hydrolab data loggers have a precision of  $\pm 0.15^{\circ}\text{C}$  and  $\pm 0.1$  ppt, respectively. To characterize the mixing relation of  $\delta^{18}\text{O}_{\text{WATER}}$  between fresh and marine waters, 15 ml samples were collected at the time the water property measurements were made. Samples of  $\delta^{13}\text{C}_{\text{DIC}}$  (dissolved inorganic carbon) were collected monthly during the 25-month period at the oyster reef to compare  $\delta^{13}\text{C}_{\text{SHELL}}$  (shell carbonate) with that of ambient water. An additional seven samples were collected at the Blackwater River boat basin each

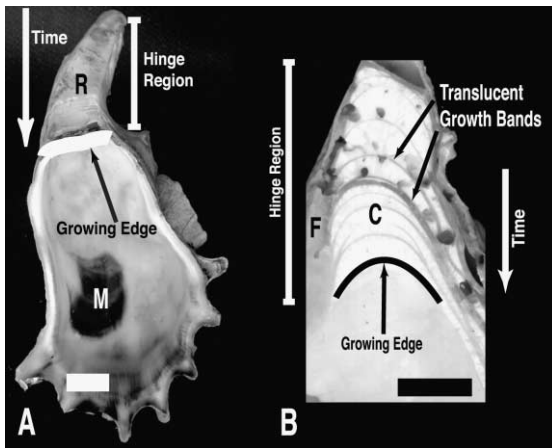


Fig. 3. Left valve of *C. virginica* both in planar (A) and cross-sectional (B) views. Bar = 1 cm. (a) Resilifer (R) is located on the surface of the hinge and is comprised of foliated calcite. Muscle scars (M) are comprised of aragonite. (b) Cross-section of left valve cut ventrally to dorsally through the resilifer perpendicular to growth. Foliated calcite (F) underneath the resilifer surface is exposed in cross-section. Chalky layer (C) contains porous calcite and dark, translucent growth bands. Pits in the shell were caused by boring algae or sponges. Foliated calcite on the resilifer surface and in cross-section as well as chalky calcite were sampled for isotopic analysis perpendicular to growth. Shell is secreted incrementally toward the bottom.

month from May to November 1999 to evaluate the composition of nearly pure meteoric water (Fig. 1). Water samples for  $\delta^{13}\text{C}$  analysis were filtered, treated with  $\text{HgCl}_2$  or zephiran chloride to eliminate metabolic activity, and sealed in impermeable 30 ml serum vials.

Values of  $\delta^{18}\text{O}_{\text{WATER}}$  were measured using an automated Finnigan  $\text{CO}_2\text{--H}_2\text{O}$  equilibration unit. Five milliliters of water were equilibrated with  $\text{CO}_2$  in an agitating water bath for a minimum of 8 h at  $15^\circ\text{C}$  and measured on a Finnigan Delta-S mass spectrometer. Data were normalized to an internal standard water and absolute values were normalized to measured values of VSMOW and VSLAP. The standard deviation for repeated measurements of the internal standard is 0.06‰. Oxygen isotope ratios are reported with respect to the VSMOW standard.

DIC was extracted in vacuo as  $\text{CO}_2$  by acidification with 100%  $\text{H}_3\text{PO}_4$  at room temperature, and  $\Sigma\text{CO}_2$  was then measured with an electronic manometer. Measurements of  $\delta^{13}\text{C}_{\text{DIC}}$  were made on a Finnigan MAT Delta-S ratio gas mass spectrometer

having a standard precision of  $\pm 0.1\%$ . Carbon isotope ratios are reported with respect to the VPDB standard.

#### 4. Shell samples

*C. virginica* specimens (BW20L1 and BW20L5) were collected live from the reef in Blackwater River in December 1997, together with water samples and measurements. We also harvested oysters from the reef at monthly intervals from January to November 1999 at the same time that water chemistry was measured and sampled (Fig. 1).

Oyster shells are composed of two asymmetrical valves that are joined at their hinges by a ligament. The right valve is flat in shape having a relatively small hinge, whereas the left valve is larger in size, concave in shape, and has a large hinge. The hinges are secreted incrementally along their margins providing a sclerochronologic record (Fig. 3). Mineralogically, oyster shells are primarily calcitic; however, aragonite is deposited in areas of muscle attachment and ligostracum, which is a thin prismatic layer that allows attachment of the ligament on the surface of the hinge (Carriker and Palmer, 1979; Fig. 3). There is a lower concentration of aragonite associated with the hinge of the left valve compared to the right valve (Carriker, 1996). The mineralogy of shell carbonate becomes important when analyzing shells isotopically because calcite and aragonite have different mineral-water fractionation factors (Romanek et al., 1992). Kent (1992) reported that during times of anaerobic respiration, oysters resorb parts of their shell to buffer decreases in pH within the shell, but that areas of resorption do not include the hinge. In this study samples were taken from the hinge of the left valve because this part of the shell is best preserved, provides a larger area (relative to the right valve) to sample, and has a relatively low amount of contained aragonite along its surface (Carriker, 1996; Custer and Doms, 1990; Kent, 1992; Kirby et al., 1998). Apart from the aragonitic ligostracum, the surface of the hinge (in particular, the central gully referred to as the resilifer) is composed of dense, foliated calcite. Cutting the shell in cross-section ventrally to dorsally through the resilifer and perpendicular to growth reveals a layer of dense, foliated calcite just under

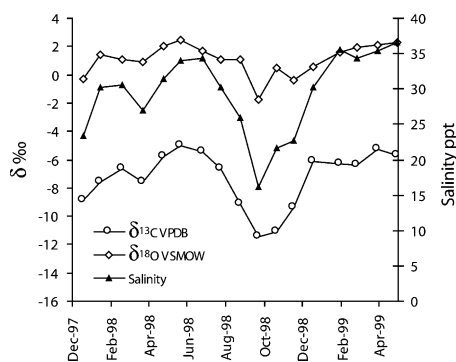


Fig. 4. Times series of  $\delta^{18}\text{O}_{\text{WATER}}$ ,  $\delta^{13}\text{C}_{\text{DIC}}$ , and salinity measured month at oyster reef from December 1997 to May 1999. Open diamonds =  $\delta^{18}\text{O}_{\text{water}}$ ; open circles represent  $\delta^{13}\text{C}_{\text{DIC}}$ ; filled triangles = salinity.

the resilifer. Below this foliated calcite is a layer containing a porous, spongy textured calcite banded by dark, translucent growth structures, referred to inclusively as the chalky layer (Carriker, 1996; Fig. 3). These three microstructural areas of the hinge (surficial foliated layer — resilifer surface, cross-sectioned foliated layer, and cross-sectioned chalky layer) were sampled within one of the shells (specimen BW20L5) to evaluate differences in isotopic composition. Comparing the foliated layers on the surface of the hinge (resilifer) and in cross-section allowed us to determine whether the close proximity of the aragonitic ligostracum affected the isotopic composition of the calcitic resilifer. The chalky layer was sampled from the cross-section. All three areas were sampled perpendicular to growth. Low-resolution sampling was accomplished using a 0.5 mm dental burr (0.5 mm intervals), yielding  $\sim 30 \mu\text{g}$  of carbonate powder. The chalky layer of specimen BW20L1 was also sampled at this resolution to investigate the temperature of growth cessation.

Selected shells that were harvested monthly (those collected in January–May, September, and November) were sampled at high-resolution along the chalky layer perpendicular to growth. High-resolution sampling ( $\sim 100\text{--}200 \mu\text{m}$  intervals) was achieved by first digitizing an image of the cross-sectioned hinge in X–Y coordinate space using the dark, translucent growth bands contained in the chalky layer as paths of reference and then interpolating paths between the foliated growth structures. This data file

was then read by a computer connected to an X–Y–Z micropositioning stage (see Dettman and Lohmann, 1995). Approximately  $30 \mu\text{g}$  of carbonate powder was collected for each sample. Both low- and high-resolution samples were roasted under vacuum at  $200^\circ\text{C}$  for 1 h, and reacted with anhydrous phosphoric acid at  $73^\circ\text{C}$  in individual reaction vessels on an on-line, automated Kiel device coupled to a Finnigan-MAT 251 mass spectrometer. Precision of the instrument is better than  $0.1\text{‰}$  for  $\delta^{13}\text{C}$  and  $\delta^{18}\text{O}$  values. Oxygen isotope ratios were corrected for  $^{17}\text{O}$  contribution (Craig, 1957) and are reported in permil units with respect to the VPDB standard.

## 5. Results and discussion

### 5.1. Water temperature, salinity, and chemistry

Water temperature at the oyster reef ranges from  $12\text{--}35^\circ\text{C}$  and varies more or less sinusoidally between winter and summer months with mean summer and winter temperature of  $31$  and  $20^\circ\text{C}$ , respectively (Fig. 2). Temperature is more variable during winter months, probably due to the passage of winter cold fronts. Salinity at the reef ranges from  $5\text{--}39$  ppt and also varies seasonally, becoming brackish during late summer through mid fall (August through November), and returning close to marine values the rest of the year. Brackish values coincide with or follow periods of increased precipitation during the seasonal summer-fall rainy season (Fig. 2). Based on salinity, the months of August through November during years 1996 and 1997 were much drier than those months during years 1998 and 1999. Conversely, precipitation data indicate that 1999 was the driest of the 4 years. However, because rainfall data from Fort Meyers, Florida is  $55$  km farther north of the study area, salinity data probably better represent weather conditions over Blackwater River drainage area.

Oxygen isotope composition of estuary water measured monthly at the oyster reef locality varies seasonally with salinity (Fig. 4). Negative  $\delta^{18}\text{O}$  values coincide with a decrease in salinity during wet months, and more positive  $\delta^{18}\text{O}$  values occur with increased salinity during the drier months. Values of  $\delta^{18}\text{O}$  across the  $12$  km transect between the Blackwater River boat basin and the Gulf of Mexico

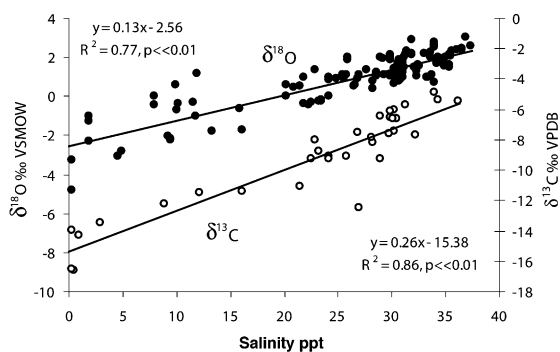


Fig. 5. Relationship between salinity and isotopic composition of water ( $p \ll 0.01$ ,  $\alpha = 0.05$ ). Filled circles =  $\delta^{18}\text{O}$ ; open circles =  $\delta^{13}\text{C}$  vs. salinity.

exhibits a linear covariant trend between meteoric (0 ppt) and marine (37 ppt) salinities, respectively (Fig. 5). The relationship between salinity and  $\delta^{18}\text{O}_{\text{WATER}}$  yielded the following least-squares regression equation ( $r^2 = 0.77$ ,  $t_s = 0.019$ ,  $t_{0.001[131]} = 3.291$ ,  $p < 0.001$ ):

$$\delta^{18}\text{O}_{\text{WATER}} = 0.13(\pm 0.01)\text{S}\%_o - 2.57(\pm 0.17) \quad (1)$$

where  $\text{S}\%_o$  is salinity (Fig. 5). This correlation describes the mixing relation of meteoric and marine end members, and calculates freshwater salinity to have an average  $\delta^{18}\text{O}_{\text{WATER}}$  value of  $-2.57\%_o$ . The most negative measured meteoric value at 0 ppt determined from the boat basin is  $-4.88\%_o$ , whereas the most positive measured value for water from the Gulf of Mexico is  $+3.00\%_o$  at 37 ppt. The oxygen isotope composition of rain water measured from one storm in July 1998 near another estuary in the Ten Thousand Islands was as negative as  $-4.69\%_o$ . Therefore, the isotopic composition of meteoric water is likely reflecting some contribution of local precipitation. Groundwater and surface runoff are potentially other contributors; however, the contribution from these sources is unknown. Surge and Lohmann (2001, in preparation) present a more detailed discussion of the chemical hydrology in this area.

A month-to-month profile of  $\delta^{13}\text{C}_{\text{DIC}}$  measured at the oyster reef varies seasonally with salinity. Like  $\delta^{18}\text{O}$ , negative values of  $\delta^{13}\text{C}_{\text{DIC}}$  coincide with decreases in salinity during the wet season, whereas more positive  $\delta^{13}\text{C}_{\text{DIC}}$  values correspond to higher salinity during dry season months (Fig. 4). Comparison

of salinity with carbon isotope composition of estuary water measured at the Blackwater River boat basin and oyster reef results in a linear covariant trend between meteoric (0 ppt) and marine-like (36 ppt) salinities, respectively (Fig. 5). The relationship between salinity and  $\delta^{13}\text{C}_{\text{DIC}}$  is described by the following least-squares regression equation ( $r^2 = 0.87$ ,  $t_s = 0.023$ ,  $t_{0.001[31]} = 3.646$ ,  $p < 0.001$ ):

$$\delta^{13}\text{C}_{\text{DIC}} = 0.27(\pm 0.02)\text{S}\%_o - 15.38(\pm 0.48) \quad (2)$$

where  $\text{S}\%_o$  is salinity (Fig. 5). Like  $\delta^{18}\text{O}_{\text{WATER}}$ , this equation represents the mixing relation between freshwater and higher salinity estuarine water. Calculated  $\delta^{13}\text{C}_{\text{DIC}}$  of water having a salinity of 0 ppt is  $-15.39\%_o$ . The most negative value of  $\delta^{13}\text{C}_{\text{DIC}}$  of freshwater at 0 ppt measured from the boat basin is  $-16.65\%_o$ . Negative values of the meteoric end member probably reflects contributions from terrestrial, atmospheric, and groundwater sources. However, the balance between these sources cannot be uniquely discriminated in this study. The most positive value measured at the reef is  $-4.98\%_o$  at 34 ppt. This value is more negative than seawater values ( $\sim 1.5\%_o$ ) at subtropical latitudes (Kroopnick, 1980). Therefore, the negative value at near-marine salinity probably reflects an equilibration with local sources of carbon.

## 5.2. Shell microstructural chemistry

We tested the hypothesis that there are no differences in the isotopic composition between microstructural areas (surface of the resilifer and foliated and chalky calcite in cross-section). It is important to understand whether there is a microstructural effect on the isotopic composition of shell carbonate before answering questions of equilibrium precipitation and temperature of growth cessation because one area may more faithfully record ambient water conditions.

To evaluate the similarity of isotopic composition between the microstructural areas, carbon and oxygen isotope composition was compared among the resilifer surface, and the chalky and foliated layers from the cross-section in shell BW20L5 (Fig. 6). Covariant trends of  $\delta^{18}\text{O}_{\text{SHELL}}$  and  $\delta^{13}\text{C}_{\text{SHELL}}$  of the three regions are statistically indistinguishable in both carbon and oxygen ( $\delta^{18}\text{O}$ : Kruskal–Wallis test statistic = 0.435;  $\delta^{13}\text{C}$ : Kruskal–Wallis test statistic = 0.333;  $\chi^2_{0.001[2]} =$

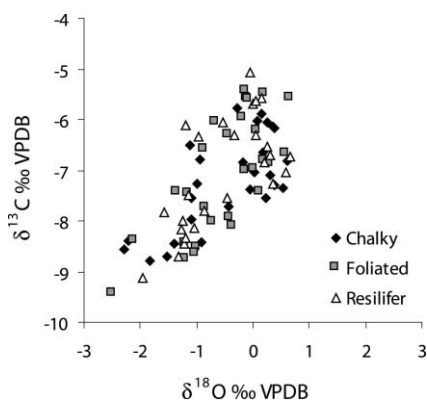


Fig. 6. Cross-plot of oxygen and carbon isotope composition of microstructural layers from shell BW20L5. Chalky calcite (black diamonds) were sampled in cross-section. Foliated calcite was sampled in cross-section (gray squares) and on the surface of the resilifer (white triangles).

13.816). All three layers have similar ranges ( $\sim 3\%$ ), minimum ( $-2$  to  $-2.5\%$ ) and maximum ( $+0.65\%$ ) values of  $\delta^{18}\text{O}$  (Table 2). Maximum and minimum  $\delta^{13}\text{C}$  values are  $\sim -5.5$  and  $\sim -9\%$ , respectively (Table 2). The chalky layer has a range of  $3\%$ , whereas foliated calcite from the resilifer and in cross-section has a  $4\%$  range in  $\delta^{13}\text{C}$ .

Given these results, it is possible to use any of these regions of the hinge for isotopic analysis. We chose to work in the chalky layer on the cross-section of the hinge. This approach allowed us to optimize temporal resolution by sampling along the maximum extension of growth and along coeval growth structures.

### 5.3. Model shell

To relate  $\delta^{18}\text{O}_{\text{SHELL}}$  and  $\delta^{13}\text{C}_{\text{SHELL}}$  to environmental conditions and to answer questions of equilibrium precipitation and growth, we calculated a predicted

profile of oxygen and carbon isotope composition for calcite precipitating in equilibrium with water conditions at the reef during the time period over which the live-collected shells were growing. This model of  $\delta^{18}\text{O}_{\text{SHELL}}$  is based on daily water temperature and salinity measurements (reduced from the hourly data set), the salinity- $\delta^{18}\text{O}_{\text{WATER}}$  relation (Eq. (1)), and the equilibrium fractionation equation for calcite and water (modified from Tarutani et al., 1969),

$$10^3 \ln \alpha_{\text{CC-W}} = 2.78 \times 10^6 T^{-2} - 2.89 \quad (3)$$

where  $T$  is temperature in Kelvin and  $\alpha_{\text{CC-W}}$  is the fractionation between calcite and water. (Fig. 6). We omitted the term that accounts for mole percent  $\text{MgCO}_3$  because *C. virginica* produces a low-magnesium calcite shell ( $0.5$ – $1.5$  mol%  $\text{MgCO}_3$ ; Lerman, 1965 and D. Surge, unpublished data). A maximum mole percent  $\text{MgCO}_3$  of  $1.5$  would amount to, at most, a  $+0.09\%$  shift in calculated  $\delta^{18}\text{O}_{\text{SHELL}}$ , which is negligible for our purposes. Moreover, we chose this temperature equation because it avoids uncertainties associated with applying a correction (subtracting  $0.20$ – $0.27\%$  from all  $\delta^{18}\text{O}_{\text{WATER}}$  values to convert from the VSMOW to VPDB scales), which is required of other temperature equations (e.g. Epstein et al., 1953; Erez and Luz, 1983). Eq. (3) yields carbonate  $\delta^{18}\text{O}$  relative to VSMOW, which we convert to the VPDB scale using Gonfiantini et al. (1995):

$$\begin{aligned} \delta^{18}\text{O}_{\text{CALCITE(VPDB)}} \\ = (\delta^{18}\text{O}_{\text{CALCITE(VSMOW)}} - 30.91) / 1.03091 \quad (4) \end{aligned}$$

Note that there are gaps (4/1–4/2/98, 4/15–5/6/98, 6/1–6/7/98, 9/23–9/30/98, 12/1/98–1/6/99, 3/7–3/10/99, 3/23–3/30/99) in the temperature and salinity data due to instrument malfunction. Gaps were filled by

Table 2  
Descriptive statistics of microstructural areas

	Resilifer		Foliated		Chalky	
	$\delta^{18}\text{O}$	$\delta^{13}\text{C}$	$\delta^{18}\text{O}$	$\delta^{13}\text{C}$	$\delta^{18}\text{O}$	$\delta^{13}\text{C}$
Mean	-0.53	-7.07	-0.51	-7.13	-0.48	-7.23
Range	2.63	4.06	3.15	4.00	2.92	3.00
Minimum	-1.97	-9.14	-2.5	-9.45	-2.30	-8.79
Maximum	0.66	-5.08	0.65	-5.45	0.62	-5.79

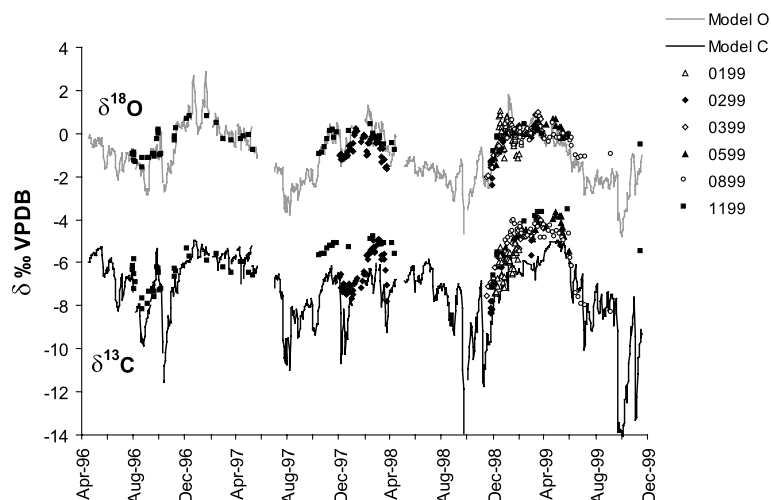


Fig. 7. Predicted model shell representing daily average calculated for the oyster reef in Blackwater River from April 1996 to November 1999 and observed shell data from that site. Gray line = predicted  $\delta^{18}\text{O}$  (above); black line = predicted  $\delta^{13}\text{C}$  (below). Symbols represent observed shell data: open triangle = Shell 0199; filled diamond = Shell 0299; open diamond = Shell 0399; filled triangle = Shell 0599; open circle = Shell 0899; filled square Shell 1199. Observed data points of shells were assigned dates based on anchoring the most recently deposited shell on the date it was collected and correlating the remaining points with the predicted carbon and oxygen isotope profile.

first calculating least-squared regression equations for measurements from the data recorder at the oyster reef and from another YSI data recorder deployed at site BW25 located  $\sim 3$  km upstream from the reef locality (temperature:  $r^2 = 0.97$ ; salinity:  $r^2 = 0.91$ ;  $p \ll 0.01$ ,  $\alpha = 0.05$ ; Fig. 1). From these equations and the data from site BW25, we predicted what the temperature and salinity would be at the oyster reef. We were not able to fill gaps in the data prior to April 1998 because the upstream data recorder was not in operation before this time.

The predicted  $\delta^{18}\text{O}_{\text{SHELL}}$  profile is more highly correlated with seasonal temperature change rather than salinity (correlation coefficients comparing  $\delta^{18}\text{O}$  of predictive model to daily temperature and salinity at the oyster reef:  $r_{T^\circ\text{C}} = -0.74$ ,  $r_{S\text{‰}} = -0.19$ ). However, because the rainy season occurs from July through November (based on atmospheric precipitation data collected between 1996–1999 at Naples and Fort Meyers, Florida by the National Oceanographic and Atmospheric Association), the late summer through fall model  $\delta^{18}\text{O}_{\text{SHELL}}$  values have prominent negative excursions that coincide with drops in salinity due to increased freshwater input (Figs. 2 and 7). Afternoon thunderstorms during this part of the year are convectional in nature and

occur on almost a daily basis, contributing tens of cm of rain per month (Fig. 2). Dips in the winter  $\delta^{18}\text{O}_{\text{SHELL}}$  values are produced by rain events associated with the passage of cold fronts. These storms produce less than 10 cm of rain monthly (Fig. 2). Therefore, the predicted  $\delta^{18}\text{O}_{\text{SHELL}}$  profile during this interval has less prominent negative excursions than those occurring in late summer/fall reflecting relatively low rainfall and near-marine salinity.

Model  $\delta^{13}\text{C}_{\text{SHELL}}$  is based on the salinity- $\delta^{13}\text{C}_{\text{DIC}}$  relation (Eq. (2)). Due to the paucity of  $\sum\text{CO}_2$  and pH measurements, we compared  $\delta^{13}\text{C}_{\text{SHELL}}$  to  $\delta^{13}\text{C}_{\text{DIC}}$  directly. This comparison is reasonable given that temperature has only a minor effect on  $\delta^{13}\text{C}$  of calcite. Therefore, we use this model to test the hypothesis that  $\delta^{13}\text{C}$  of oyster shells and salinity are correlated.

#### 5.4. Observed vs. Predicted shell

The observed  $\delta^{18}\text{O}_{\text{SHELL}}$  and  $\delta^{13}\text{C}_{\text{SHELL}}$  records of the last 3–7 mm of growth from selected shells collected each month were compared to the predictive models (Figs. 7 and 8). Comparing the covariance of  $\delta^{18}\text{O}$  and  $\delta^{13}\text{C}$  between model and observed shells illustrates a correspondence between predicted and observed sample populations, with one exception

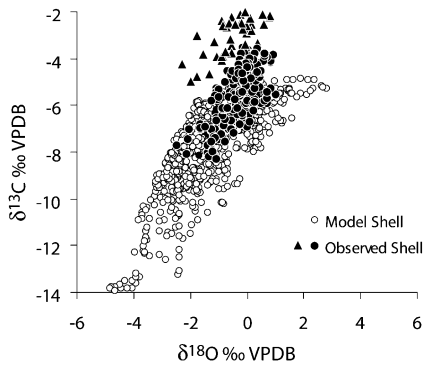


Fig. 8. Covariance of  $\delta^{18}\text{O}$  and  $\delta^{13}\text{C}$  comparing predicted and observed shells. Open circles are calculated points based on the model and filled symbols are observed data points. Filled triangles represent shell 0499, and filled circles represent the pooled data from the remaining shells.

(Fig. 8). Values of  $\delta^{13}\text{C}$  from Shell 0499 collected in April 1999 do not overlap with either the predictive model or with population of other live-collected shells. We interpret this offset as possibly non-equilibrium precipitation. Therefore, given its potential disequilibrium, we excluded Shell 0499 from further analysis in this study. Of the observed, live-collected shells that correspond with the predictive model, some  $\delta^{13}\text{C}_{\text{SHELL}}$  values are more positive than those from the predictive model. Moreover, the most negative  $\delta^{18}\text{O}$  and  $\delta^{13}\text{C}$  values from the model shell are not represented in the observed shells. Profiles of isotopic composition of the model and observed shells relative to time (i.e. seasons) were compared to evaluate the nature of these offsets (Fig. 7).

Comparing shell data to model data relative to time required assignment of dates to individual data points from observed shells. The harvest date of each live-collected shell served to anchor the last increment of growth onto the model (i.e. the final increment of shell deposited should record the ambient conditions prior to the time of harvest). The remaining observed data points for all shells were plotted against the model using the predicted  $\delta^{18}\text{O}$  and  $\delta^{13}\text{C}$  as correlation tools, with some sections of the measured shells requiring rescaling (stretching) to account for differential growth rates or periods of no growth. In other words, we simultaneously aligned  $\delta^{18}\text{O}$  and  $\delta^{13}\text{C}$  of the observed shells to  $\delta^{18}\text{O}$  and  $\delta^{13}\text{C}$  of the model to

achieve a best-fit solution. Uniform rescaling of the shell is inappropriate for *C. virginica* because its shell is morphologically plastic (i.e. shell shape and growth rate varies within and between individuals depending on environmental factors, such as substrate, predation pressure, food availability, etc. (e.g. Galstoff, 1964; Palmer and Carriker, 1979; Carriker, 1996 and references cited therein). Despite the morphologic plasticity exhibited by *C. virginica*, the high-resolution sampling reduced time averaging to the daily to weekly scale and allowed evaluation of equilibrium precipitation of shell carbonate.

Oxygen isotope composition of shell carbonate follows the expected equilibrium trend in all of the shells, though there are slight excursions off of equilibrium in portions of some of the shells. For example, the most recent portion of shell 0199 collected in January 1999 deviates negatively from equilibrium by  $\sim 0.75\text{‰}$ . If equilibrium precipitation is assumed in this shell, then an overestimation in temperature of  $\sim 4^\circ\text{C}$  would result. Carbon isotope composition of all shells follows the general trend of equilibrium precipitation, although there is a positive offset of  $\sim 1\text{‰}$  during colder months. Shell deposited during warmer months is more closely aligned to predicted values. The shell collected in November 1999 (shell 1199) follows predicted  $\delta^{13}\text{C}$  in its first year of growth. These results suggest that  $\delta^{13}\text{C}_{\text{SHELL}}$  is generally correlated with salinity; however, there is some contribution of metabolic carbon (e.g. from food carbon, respiration, or faster growth rates that may vary seasonally). Despite a possible metabolic contribution, carbon follows the general salinity trend (Fig. 2), and therefore, it can be used as a proxy for salinity if corrected for the  $1\text{‰}$  offset in winter months. Given the anomalous positive offset of shell 0499, it is important to analyze multiple shells when reconstructing past environments to potentially identify shells that may be recording anomalous conditions.

Closer inspection of shells that follow the models reveals seasonal changes in shell growth. The observed  $\delta^{18}\text{O}$  values do not represent the most negative predicted values suggesting that *C. virginica* living in southwest Florida does not deposit shell during the hottest part of the year. Cessation of growth may reflect the onset of gametogenesis which is triggered by a rapid increase in temperature (Galstoff, 1964; Kennedy et al., 1996). Various workers note

that oysters from northwestern Florida spawn from April through September when temperature is warmest (Butler, 1965; Hayes and Menzel, 1981; Volety et al., 1999). Given our observations, the cause of growth cessation (temperature vs. gametogenesis) cannot be decoupled in this case and does not affect the utility of oyster shell chemistry as a tool for environmental reconstruction. Regardless of the cause of shell growth cessation, oysters in southwest Florida slow or cease shell growth from late summer

through fall. The phenomenon of summer cessation has also been reported in the hard clam *Mercenaria campechiensis* which inhabits this region (Jones and Quitmyer, 1996).

We estimated cessation temperature using an approach that does not rely on date assignments. This approach assumes that the most negative  $\delta^{18}\text{O}$  values occurred at the warmest temperatures. Daily averages of salinity and temperature measured at the oyster reef in Blackwater River were plotted monthly for years 1996–1999. These years cover the period of shell growth for all specimens sampled for isotopic analysis. Lines of equilibrium  $\delta^{18}\text{O}_{\text{CALCITE}}$  values (isolines) were calculated based on water temperature and the salinity- $\delta^{18}\text{O}_{\text{WATER}}$  relation and then contoured every 0.5‰ in temperature/salinity space (Fig. 9A). Assuming continuous annual growth,  $\delta^{18}\text{O}$  of shell carbonate can be tracked month to month throughout the year. For example, a shell growing during year 1997 would precipitate the most positive  $\delta^{18}\text{O}$  in January when temperature is coldest and salinity is close to marine values (Fig. 9A). As temperature warms from winter to spring, shell  $\delta^{18}\text{O}$  becomes more negative. The onset of the rainy season starting around July produces yet more negative  $\delta^{18}\text{O}_{\text{SHELL}}$ . As the input of freshwater diminishes (approaching November),  $\delta^{18}\text{O}$  shell becomes more positive with decreasing temperature and increasing salinity. By comparing the most negative  $\delta^{18}\text{O}$  of an observed shell to the isolines, we identified the possible temperatures and salinities that could have produced a shell of a given oxygen isotopic composition.

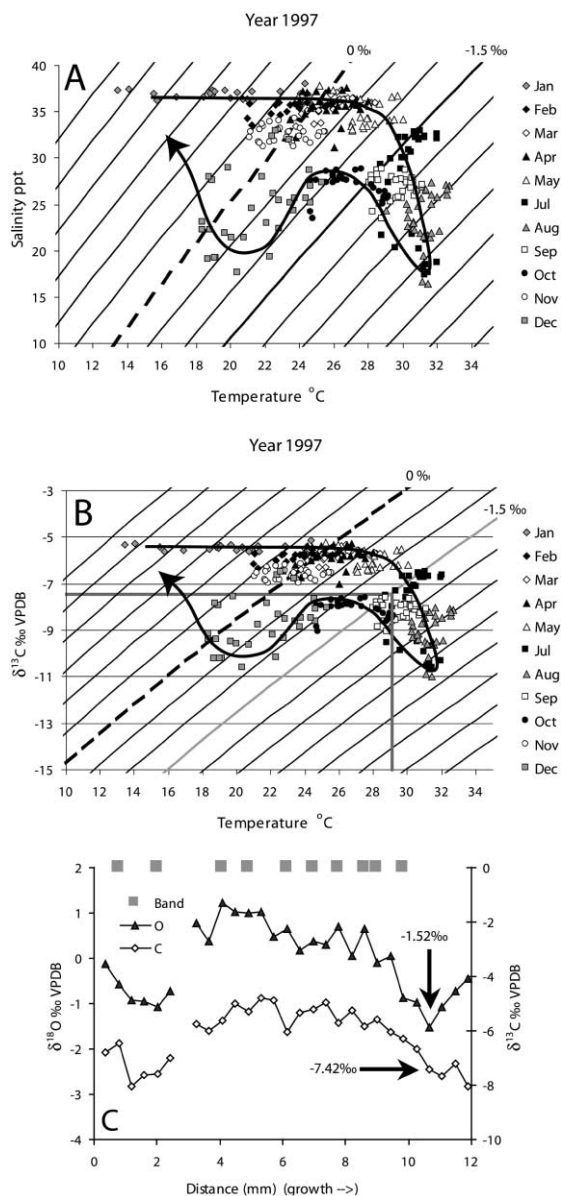


Fig. 9. Range of temperature and salinity that can produce a shell of a particular oxygen isotopic composition. Symbols are temperature and salinity measured at the reef and reduced to daily averages from the hourly data set. Gray diamonds = January; black diamonds = February; white diamonds = March; black triangles = April; white triangles = May; no data for June; black squares = July; gray triangles = August; white squares = September; black circles = October; white circles = November; and gray squares = December. (A) Temperature and salinity for year 1997 overlain by diagonally contoured isolines (lines of equilibrium  $\delta^{18}\text{O}_{\text{SHELL}}$ ). Dashed line is 0‰ and black line is -1.5‰. (B) Temperature and  $\delta^{13}\text{C}_{\text{SHELL}}$  for year 1997 overlain by diagonally contoured isolines.  $\delta^{13}\text{C}_{\text{DIC}}$  substituted for salinity. Dashed line is 0‰ and black line is -1.5‰. (C)  $\delta^{18}\text{O}$  (above) and  $\delta^{13}\text{C}$  (below) profiles of shell BW20L1 collected in December 1997 identifying shell deposited during the warmest part of that year. Gray bar identifies location of translucent growth bands.

Table 3

Estimates of temperature of growth cessation calculated using isolines and measured daily temperature and salinity data. Note that specimen 0499 was excluded from this analysis because of probable disequilibrium precipitation of  $\delta^{13}\text{C}_{\text{SHELL}}$

Shell/Year	$\delta^{18}\text{O}_{\text{shell}}$ (‰ VPDB)	$\delta^{13}\text{C}_{\text{shell}}$ (‰ VPDB)	Temperature estimate (°C)
<b>BW20L1</b>			
Fall 1996	– 1.07	– 7.59	26
Fall 1997	– 1.52	– 7.42	29
<b>BW20L5</b>			
Fall 1997	– 2.3	– 8.57	30.5
<b>299</b>			
Fall 1998	– 2.43	– 7.77	32
<b>899</b>			
Fall 1999	– 1.14	– 8.04	26
<b>1199</b>			
Fall 1996	– 1.62	– 8.22	28
Fall 1997	– 1.01	– 6.69	28.5
Fall 1998	– 0.84	– 6.63	28
Fall 1999	– 0.57	– 5.53	27

To better constrain the temperature of precipitation, we employed  $\delta^{13}\text{C}$  as a tracer for salinity. To facilitate this, we recast salinity in terms of  $\delta^{13}\text{C}_{\text{DIC}}$  given that  $\delta^{13}\text{C}_{\text{SHELL}}$  closely aligned with the carbon isotope composition of DIC during warmer months (Figs. 7 and 9B). For example, specimen BW20L1 was collected in December 1997 (Fig. 9C). Therefore, its most negative  $\delta^{18}\text{O}_{\text{SHELL}}$  value (–1.52‰) and corresponding  $\delta^{13}\text{C}$  value (–7.42‰) likely record growth during the warm part of the year. The common point on the isolines that corresponds to these delta values identifies the highest temperature of growth recorded in the shell as  $\sim 29^\circ\text{C}$ . By following this procedure using the most negative  $\delta^{18}\text{O}_{\text{SHELL}}$  values and corresponding  $\delta^{13}\text{C}$  values for selected specimens, the temperature above which *C. virginica* does not precipitate shell is constrained to  $\sim 28(\pm 2)^\circ\text{C}$  (Table 3). We could not use shells 0199, 0399, and 0599 because the interval sampled through the shell captured only a portion of the year that did not include the period of growth cessation. Furthermore, we excluded shell 0499 from this analysis given the probable disequilibrium precipitation with respect to carbon. Nonetheless, our estimation of the temperature of growth cessation is in general agreement with that reported by Kirby et al. (1998).

### 5.5. Shell morphology: foliated growth bands

Given the seasonal nature of the observed profiles of isotopic composition of shell carbonate (broad peaks (winters) and truncated valleys (summers)) and seasonal changes in growth (cessation), we hypothesized that the dark, translucent bands within the chalky layer visible on the cross-section of the hinge might serve as sclerochronologic markers (independent identification of seasonal growth) (Fig. 9C). Other bivalves form similar growth features that correlate with periods of hibernation, gametogenesis, tides, or other stresses (e.g. Jones, 1983; Jones, 1996; Jones and Quitmyer, 1996). In contrast to the findings reported by Andrus and Crowe (2000), we find no seasonal pattern (when compared to the profiles of isotopic composition of shell carbonate) with respect to the formation of translucent growth bands (Fig. 9C). Bands were also characterized hierarchically (thick vs. thin) to examine any tidal or lunar relationship. Date assignments allowed comparison of band location with tides, particularly spring tides, and lunar cycles. No relationships were observed. Therefore, translucent growth bands cannot serve as independent proxies of seasons or tides. Perhaps the chalky layers precipitated between the translucent bands are energetically more economical to produce or correspond to some metabolic change not yet identified. Alternatively, the translucent bands may serve a functional purpose to the structure and strength of the shell rather than as a reflection of seasonal patterns of growth.

In a previous study, Kirby et al. (1998) suggested that other morphologic features (concave up and concave down ridges on the hinge surface of the left valve) found on *C. virginica* have seasonal significance. We found no such morphologic features on any of the oysters collected within Rookery Bay Reserve. It is likely that given the degree of ecophenotypic variation inherent in oysters, morphologic features are not reliable indicators of seasonal growth patterns despite the incremental process of shell deposition.

## 6. Summary

The hinge of the left valve of *C. virginica* can be used to reconstruct past estuarine environments once

the chemistry of its shell is understood. The microstructural layers in cross-section (chalky and foliated) and on the surface of the resilifer (foliated) from the hinge on the left valve of *C. virginica* are not isotopically different from each other. Therefore, any of these layers can be used for environmental reconstruction. We chose to focus our investigations on the chalky layer because this region exhibits maximum shell extension allowing for high-resolution sampling.

To test the hypothesis that *C. virginica* precipitates its shell in isotopic equilibrium with ambient water, we constructed predicted  $\delta^{18}\text{O}$  and  $\delta^{13}\text{C}$  models for calcite against which to compare the actual isotopic composition of oyster shells growing over that time period. Model  $\delta^{18}\text{O}_{\text{SHELL}}$  is based on temperature and the salinity- $\delta^{18}\text{O}_{\text{WATER}}$  relation, and model  $\delta^{13}\text{C}_{\text{SHELL}}$  is equivalent to predicted  $\delta^{13}\text{C}_{\text{DIC}}$  based on the salinity- $\delta^{13}\text{C}_{\text{DIC}}$  relation. We chose to compare  $\delta^{13}\text{C}_{\text{SHELL}}$  to  $\delta^{13}\text{C}_{\text{DIC}}$  given the paucity of pH and  $\Sigma\text{CO}_2$  data. By comparing the oxygen and carbon isotope composition of shell carbonate sampled perpendicular to growth through the chalky layer with the predicted calcite models, we determined that *C. virginica* precipitates its shell near isotopic equilibrium. However, deviations from equilibrium can occur in both  $\delta^{18}\text{O}$  and  $\delta^{13}\text{C}$ .  $\delta^{18}\text{O}$  is occasionally offset from the predicted equilibrium by  $\sim 0.75\%$ . This offset can hamper environmental reconstruction by overestimating temperature by  $\sim 4^\circ\text{C}$ .  $\delta^{13}\text{C}_{\text{SHELL}}$  follows the general trend of predicted  $\delta^{13}\text{C}_{\text{DIC}}$ ; however, it is offset from  $\delta^{13}\text{C}_{\text{DIC}}$  by  $+1\%$  during cold months. Therefore, if the most positive  $\delta^{13}\text{C}_{\text{SHELL}}$  values from shell that formed during winter months are corrected for the  $1\%$  positive offset,  $\delta^{13}\text{C}_{\text{SHELL}}$  can be used as a proxy for salinity assuming the relationship between salinity and  $\delta^{13}\text{C}_{\text{DIC}}$  has not changed through time. This assumption may not always hold true. Given the occasional disequilibrium precipitation in carbon (e.g. the anomalously positive offset of shell 0499), it is important to analyze multiple shells to identify anomalous values.

Assuming date assignments of the observed isotopic composition of shell carbonate are correct, *C. virginica* grows its shell from October–November through June–July when water temperature falls below  $\sim 28^\circ\text{C}$  and in the absence of gametogenesis. Given the coincidence of the onset of gametogenesis with rapid increase in temperature, we cannot

uniquely determine whether biologic or external physical factors control the cessation in shell growth. Finally, there is no seasonal, tidal, or lunar correspondence between dark, translucent growth bands within the chalky layer and isotopic composition. This finding contrasts the conclusions of Andrus and Crowe (2000). Other morphologic features, in particular concave up/concave down ridges suggested by Kirby et al. (1998) to have seasonal significance, were not observed in any of the oysters studied here. Therefore, translucent banding and concave ridges are not reliable independent proxies of seasons. This conclusion is not surprising given the extreme variability of shell formation inherent to oysters.

### Acknowledgements

We appreciate the analytical assistance of Lora Wingate. This manuscript was greatly improved by discussions with and comments by Bruce Wilkinson, Tom Baumiller, Mike Savarese, and Diarmaid Ó Foighil. We thank Peter Swart and an anonymous reviewer for their helpful comments and suggestions. Special thanks to Karl Flessa for encouragement and discussions in the early stages of this project. Partial funding provided by NSF (grant #EAR-9809374) to KCL and by NERRS/NOAA Graduate Research Fellowship (award #NA87OR0465); Rackham Graduate Summer Research Scholarship and Scott Turner Award, University of Michigan; Geological Society of America; Lerner-Gray Fund for Marine Research, American Museum of Natural History; Chevron Fund, University of Arizona; and Conchologists of America to DS. This project would not have been possible without the help and dedication of FORB, especially Sam Stamper, Dianne Cole-Bronczyk, and Heather Stoffel.

### References

- Andrus, C.F.T., Crowe, D.E., 2000. Geochemical analysis of *Crassostrea virginica* as a method to determine season of capture. *Journal of Archaeological Science* 27, 33–42.
- Bemis, B.E., Geary, D.H., 1996. The usefulness of bivalve stable isotope profiles as environmental indicators: data from the eastern Pacific Ocean and the southern Caribbean Sea. *Palaios* 11, 328–339.
- Butler, P.A., 1965. Reactions of estuarine mollusks to some

- environmental factors. (eds.), Biological Problems in Water Pollution, U.S.H.E.W. Public Health Service, pp. 92–104.
- Carriker, M.R., 1996. Chapter 3. The Shell and Ligament. In: Kennedy, V.S., Newell, R.I.E., Eble, A.F. (Eds.), The Eastern Oyster, *Crassostrea virginica*. Maryland Sea Grant, 105 pp.
- Carriker, M.R., Palmer, R.E., 1979. A new mineralized layer in the hinge of the oyster. *Science* 206, 627–629.
- Craig, H., 1957. Isotopic standards for carbon and oxygen and correction factors for mass-spectrometric analysis of carbon dioxide. *Geochimica et Cosmochimica Acta* 12, 133–149.
- Custer, J.F., Doms, K.R., 1990. Analysis of microgrowth patterns of the American oyster (*Crassostrea virginica*) in the middle Atlantic region of eastern North America: archaeological applications. *Journal of Archaeological Science* 17, 151–160.
- Dettman, D.L., Lohmann, K.C., 1995. Microsampling carbonates for stable isotope and minor element analysis: physical separation of samples on a 20 micrometer scale. *Journal of Sedimentary Research A65*, 566–569.
- Dettman, D.L., Reische, A.K., Lohmann, K.C., 1999. Controls on the stable isotope composition of seasonal growth bands in aragonitic fresh-water bivalves (unionidae). *Geochimica et Cosmochimica Acta* 63, 1049–1057.
- Epstein, S., Buchsbaum, R., Lowenstam, H.A., Urey, H.C., 1953. Revised carbonate water isotopic temperature scale. *Geological Society of America Bulletin* 2, 417–425.
- Erez, J., Luz, B., 1983. Experimental paleotemperature equation for planktonic foraminifera. *Geochimica et Cosmochimica Acta* 47, 1025–1031.
- Galstoff, P.S., 1964. Morphology and structure of shell. The America oyster *Crassostrea virginica*. Galstoff, P.S. (Ed.), *Fishery Bulletin*, 21–27 chapter II.
- Gonfiantini, R., Stichler, W., Rozanski, K., 1995. Standards and intercomparison materials distributed by the International Atomic Energy Agency for stable isotope measurements. Reference and intercomparison materials for stable isotopes of light elements, I.A.E.A., pp. 13–29.
- Hayes, P.F., Menzel, R.W., 1981. The reproductive cycle of early setting *Crassostrea virginica* in the northern Gulf of Mexico, and its implications for population recruitment. *Biological Bulletin* 160, 80–88.
- Jones, D.S., 1983. Sclerochronology: reading the record of the molluscan shell. *American Scientist* 71, 384–391.
- Jones, D.S., 1996. Playing back skeletal recordings. *Palaaios* 11, 293–294.
- Jones, D.S., Allmon, W.D., 1995. Records of upwelling, seasonality and growth in stable-isotope profiles of Pliocene mollusk shells from Florida. *Lethaia* 28, 61–74.
- Jones, D.S., Quitmyer, I.R., 1996. Marking time with bivalve shells: oxygen isotopes and season of annual increment formation. *Palaaios* 11, 340–346.
- Jones, D.S., Williams, D.F., Arthur, M.A., Krantz, D.E., 1984. Interpreting the paleoenvironmental, paleoclimatic and life history records in mollusc shells. *Geobios, Mém. Spécial* 8, 333–339.
- Kennedy, V.S., Newell, R.I.E., Eble, A.F. 1996. The Eastern Oyster *Crassostrea virginica*. Maryland Sea Grant.
- Kent, B.W., 1992. Making Dead Oysters Talk: Techniques for Analyzing Oysters from Archaeological Sites. Maryland Historical and Cultural Publications, Crownsville, MD.
- Kirby, M.X., Soniat, T.M., Spero, H.J., 1998. Stable isotope sclerochronology of Pleistocene and Recent oyster shells (*Crassostrea virginica*). *Palaaios* 13, 560–569.
- Kjerfve, B., 1989. Estuarine geomorphology and physical oceanography. In: Day, J., Hall, C., Kemp, M., Yanezz-Arancibia, A. (Eds.), *Estuarine Ecology*. Wiley, New York, pp. 47–78.
- Klein, R.T., Lohmann, K.C., Thayer, C.W., 1996a. Bivalve skeletons record sea-surface temperature and  $\delta^{18}\text{O}$  via Mg/Ca and  $^{18}\text{O}/^{16}\text{O}$  ratios. *Geology* 24, 415–418.
- Klein, R.T., Lohmann, K.C., Thayer, C.W., 1996b. Sr/Ca and  $^{13}\text{C}/^{12}\text{C}$  ratios in skeletal calcite of *Mytilus trossulus*: covariation with metabolic rate, salinity, and carbon isotopic composition of seawater. *Geochimica et Cosmochimica Acta* 60, 4207–4221.
- Kroopnick, P., 1980. The distribution of  $^{13}\text{C}$  in the Atlantic ocean. *Earth and Planetary Science Letters* 49, 469–484.
- Lerman, A., 1965. Strontium and magnesium in water and in *Crassostrea* calcite. *Science* 150, 745–751.
- McIvor, C.C., Smith III, T.J., 1995. Differences in the crab fauna of mangrove areas at a southwest Florida and a northeast Australia location: implications for leaf litter processing. *Estuaries* 18, 591–597.
- Mook, W.G., 1971. Paleotemperatures and chlorinities from stable carbon and oxygen isotopes in shell carbonate. *Palaeogeography, Palaeoclimatology, Palaeoecology* 9, 245–263.
- Palmer, R.E., Carriker, M.R., 1979. Effects of cultural conditions on morphology of the shell of the oyster *Crassostrea virginica*. *Proceedings of the National Shellfisheries Association* 69, 58–72.
- Romanek, C.S., Grossman, E.L., Morse, J.W., 1992. Carbon isotopic fractionation in synthetic aragonite and calcite: effects of temperature and precipitation rate. *Geochimica et Cosmochimica Acta* 56, 419–430.
- Spero, H.J., 1990. Evidence for seasonal low-salinity surface waters in the Gulf of Mexico over the last 16,000 years. *Paleoceanography* 5, 963–975.
- Surge, D.M., Lohmann, K.C., 2001. Temporal and spatial differences in salinity and water chemistry in SW Florida estuaries: effects of human-impacted watersheds. *Estuaries*, in preparation.
- Swart, P.K., Dodge, R.E., Hudson, H.J., 1996. A 240-year stable oxygen and carbon isotopic record in a coral from South Florida: implications for the prediction of precipitation in southern Florida. *Palaaios* 11, 362–375.
- Tarutani, T., Clayton, R.N., Mayeda, T.K., 1969. The effect of polymorphism and magnesium substitution on oxygen isotope fractionation between calcium carbonate and water. *Geochimica et Cosmochimica Acta* 33, 987–996.
- Volety, A.K., Winstead, J.T., Fisher, W.S., 1999. Influence of seasonal factors on oyster hemocyte killing of vibrio parahaemolyticus. *Journal of Shellfish Research* 18, 323.